Proceedings of the Institute of Acoustics

FLOW NOISE

A P Dowling

Cambridge University Engineering Department, Trumpington Street, Cambridge, CB2 1PZ

1. INTRODUCTION

A passive sonar system aims to detect and analyse weak sounds emanating from a distant source. However, the sonar is situated in a relatively noisy environment. When the vessel is in motion, the unsteady pressures generated by its turbulent boundary layer are a major source of noise, which is usually referred to as 'flow noise'.

Sound from a distant source arrives at the sonar array in the form of a plane wave travelling with the sound speed. For a general incidence angle this wave produces disturbances which travel supersonically over the sonar surface. The surface wave speed may be determined from a wavenumber-frequency decomposition of the pressures measured by the array, thus determining the direction of the source. It is therefore particularly inconvenient if the flow noise pressure spectrum has any strong peaks with supersonic phase velocities, since these can be interpreted falsely as an incoming signal.

In Section 2 we review some classical results. Figure 1 shows the typical form of $\tilde{P}_R(k_1, k_2, \omega)$, the wavenumber-frequency decomposition of flow noise on a rigid surface with normal in the 3-direction. There are two main peaks. The maximum occurs in the convective regime, which for a turbulent boundary-layer flow in the 1-direction means k_1 of order $-\omega/U_c$ and k_2 small. U_c denotes a typical eddy convection velocity. The second peak is in the vicinity of the acoustic wavenumber where k, the modulus of the vector $\underline{k} = (k_1, k_2)$, is equal to ω/c_0. For highly supersonic modes with very low values of k, the surface pressure spectrum becomes 'wavenumber white', that is almost independent of k.

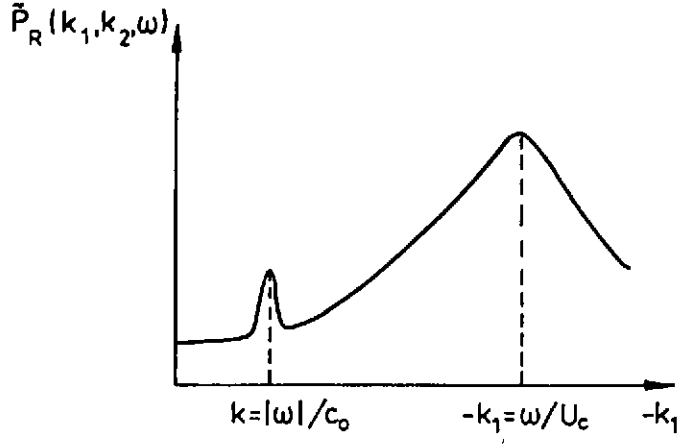

Figure 1 The wavenumber-frequency decomposition of flow noise on a rigid surface

The convective region has been considered by Corcos (1963), and is discussed in detail by Willmarth (1975) in a review article. In underwater problems, where flow Mach numbers are so small, the convective spectral components have a low subsonic surface phase speed and are essentially incompressible. The level of the pressure spectrum in the convective regime is typically some 40dB larger than that near $\underline{k} = \underline{0}$. However, we will see in §3 that the amplitude of perturbations with low, subsonic phase speeds is reduced very effectively by placing a 'dome' over the surface. The spectral elements in the acoustic regime are not attenuated in this way and there is a need to predict their level and to investigate how they might be reduced. These modes have phase speeds faster than the speed of sound and their behaviour is dominated by compressible effects (Ffowcs Williams 1965).

In §4, the compressible theory is extended to include the effects of the mean-flow profile in the turbulent boundary layer. It is found that this is particularly important when there is a dome present. The peak in the acoustic regime is enhanced for downstream propagating modes ($-k_1/\omega$ negative), but reduced for upstream propagating modes (positive k_1/ω), by the presence of the mean flow.

The wavelengths associated with spectral elements with supersonic phase speeds are so long that fluid loading can be important even on quite massive surfaces. The effects of finite surface impedance are considered in §5. Surface compliance

is found to introduce new peaks into the surface pressure spectrum. The effectiveness of surface damping and coating treatments at controlling these peaks will be discussed. Finally in §6, the effect of finite surface size is investigated. The boundaries of a flexible surface provide an inhomogeneity at which scattering from the convective peak into low wavenumbers could take place.

2. THE HARD WALL PRESSURE SPECTRUM

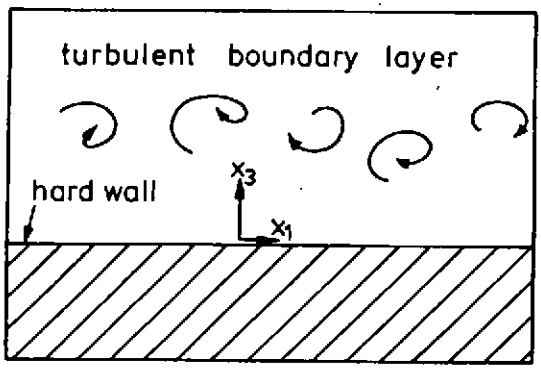

Figure 2 A turbulent boundary layer over a hard wall

Consider the geometry illustrated in Figure 2. The hard surface, $x_3 = 0$, has a turbulent boundary-layer flow over it, and we want to obtain predictions for the unsteady surface pressures. The spectral elements with supersonic surface phase velocities are of particular interest. These are essentially sound waves generated by turbulence within the boundary layer, and their strength can be determined by solving Lighthill's equation (Lighthill 1952):

$$\frac{\partial^2 p'}{\partial t^2} - c_0^2 \nabla^2 \rho' = \frac{\partial^2 T_{ij}}{\partial x_i \, \partial x_j}. \qquad (2.1)$$

This equation is just a way of rewriting the Navier-Stokes equation, which emphasizes the rôle of nonlinear fluctuations as a source of sound. ρ' denotes the density perturbation and c_0 is the speed of sound. In a high Reynolds number flow where viscous stresses are negligible, Lighthill's quadrupole source,

T_{ij}, is equal to $\rho v_i v_j + (p' - c_0^2\rho')\,\delta_{ij}$ where $\underline{v}$ is the particle velocity, ρ is the density and p' denotes pressure perturbations. In a low Mach number isentropic flow, p' is equal to $c_0^2\rho'$ and the source term reduces to the Reynolds stresses $\rho v_i v_j$. If we neglect, for now, the mean boundary-layer flow (this point is addressed in §4) $\rho v_i v_j$ is only non-zero in regions of turbulent activity and vanishes outside the boundary layer.

We are particularly interested in the spectra of the fluctuations and so it is natural to introduce Fourier transforms,

$$\tilde{\rho}(x_3, \underline{k}, \omega) = \int \rho\,(\underline{x}, t)\, e^{i k_\alpha x_\alpha + i\omega t}\, d^2\underline{k}\, d\omega\,, \tag{2.2}$$

where α is summed over 1 and 2. In terms of the transformed coordinates, equation (2.1) becomes

$$\frac{\partial^2\tilde{\rho}}{\partial x_3^2} + \gamma^2\tilde{\rho} = \frac{1}{c_0^2}\left(k_\alpha k_\beta \tilde{T}_{\alpha\beta} + 2ik_\alpha \frac{\partial\tilde{T}_{\alpha 3}}{\partial x_3} - \frac{\partial^2\tilde{T}_{33}}{\partial x_3^2}\right). \tag{2.3}$$

$\tilde{T}_{ij}\,(x_3, \underline{k}, \omega)$ is the Fourier transform of $T_{ij}\,(\underline{x}, t)$ and α, β are to be summed over 1 and 2. $\gamma = (\omega^2/c_0^2 - k^2)^{1/2}$ with the sign of the square-root chosen such that when γ is real it has the same sign as ω and when γ is purely imaginary Imγ is positive.

The hard wall boundary condition is

$$\frac{\partial\tilde{\rho}}{\partial x_3} = 0 \text{ on } x_3 = 0\,. \tag{2.4}$$

It is a straightforward matter to solve the ordinary differential equation (2.3) subject to the boundary condition (2.4) and the radiation condition at infinity. In particular, for $x_3 = 0$ we obtain

$$\tilde{p}(0, \underline{k}, \omega) = c_0^2\,\tilde{\rho}(0, \underline{k}, \omega) = \frac{d_i d_j}{i\gamma}\int_0^\infty \tilde{T}_{ij}\,(y_3, \underline{k}, \omega)\, e^{i\gamma y_3}\, dy_3 \tag{2.5}$$

where $d_\alpha = k_\alpha$, for $\alpha = 1$ or 2, and $d_3 = \gamma$.

FLOW NOISE

The power spectral density of the surface pressure, $\tilde{P}_R(\underline{k}, \omega)$, is the Fourier transform of the autocorrelation:

$$\tilde{P}_R(\underline{k}, \omega) = \int \overline{p'(x_1, x_2, 0, t)\, p'(x_1 + \Delta_1, x_2 + \Delta_2, 0, t + \tau)}\, e^{i\underline{k}_a \underline{\Delta}_a + i\omega\tau}\, d^2\underline{\Delta}\, d\omega, \qquad (2.6)$$

where the overbar denotes an ensemble average. If the turbulence is statistically stationary and homogeneous in the 1 and 2 directions, $\tilde{P}_R(\underline{k}, \omega)$ is related simply to $\tilde{p}(0, \underline{k}, \omega)$ (see Dowling and Ffowcs Williams, 1983, Chapter 10) by

$$\tilde{P}_R(\underline{k}, \omega) = \frac{1}{(2\pi)^3} \int \overline{\tilde{p}^*(0, \underline{k}, \omega)\, \tilde{p}(0, \underline{k}', \omega')}\, d^2\underline{k}'\, d\omega' \qquad (2.7)$$

The star denotes a complex conjugate. Substitution for $\tilde{p}(0, \underline{k}, \omega)$ from equation (2.5) gives

$$\tilde{P}_R(\underline{k}, \omega) = \frac{d_i^* d_j^* d_k d_l}{(2\pi)^3 \gamma^* \gamma'} \int \overline{\tilde{T}_{ij}^*(y_3, \underline{k}, \omega)\, \tilde{T}_{kl}(y_3', \underline{k}', \omega')}\, e^{i(\gamma^* y_3 - \gamma' y_3')}\, dy_3\, dy_3' \qquad (2.8)$$

By making use of the homogeneity of the turbulence again, we can write

$$\overline{\tilde{T}_{ij}^*(y_3, \underline{k}, \omega)\, \tilde{T}_{kl}(y_3', \underline{k}', \omega')} = (2\pi)^3 \delta(\underline{k} - \underline{k}')\, \delta(\omega - \omega')\, \bar{\Pi}_{ijkl}(y_3, y_3', \underline{k}, \omega), \qquad (2.9)$$

where $\bar{\Pi}_{ijkl}(y_3, y_3', \underline{k}, \omega)$ is the cross-power spectral density of the quadrupole source strengths,

$$\bar{\Pi}_{ijkl}(y_3, y_3', \underline{k}, \omega) = \int \overline{T_{ij}(\underline{y}, t)\, T_{kl}(y_1 + \Delta_1, y_2 + \Delta_2, y_3', t + \tau)}\, e^{i\underline{k}_a \underline{\Delta}_a + i\omega\tau}\, d^2\underline{\Delta}\, d\tau. \qquad (2.10)$$

When equation (2.9) is used in (2.8) we obtain

$$\tilde{P}_R(\underline{k}, \omega) = \frac{d_i^* d_j^* d_k d_l}{M^2} \int \bar{\Pi}_{ijkl}(y_3, y_3', \underline{k}, \omega)\, e^{i(\gamma^* y_3 - \gamma' y_3')}\, dy_3\, dy_3'. \qquad (2.11)$$

This result relates the wall-pressure spectrum to the Reynolds stresses in the turbulent boundary layer, and was first derived by Ffowcs Williams (1965). Equation (2.11) is in a useful form because, although very little is known about the structure of the turbulent source terms T_{ij}, it is possible to make some reasonable assumptions about the behaviour of their spectral functions, $\bar{\Pi}_{ijkl}$. As argued by Bergeron (1973), who uses a matching argument, we expect the source functions $\bar{\Pi}_{ijkl}$ to have a Taylor series about $\underline{k} = \underline{0}$. Hence, in order to investigate

the surface pressure in the low wavenumber regime, we can replace $\tilde{T}_{ijkl}(y_3, y_3', \underline{k}, \omega)$ in (2.11) by $\tilde{T}_{ijkl}(y_3, y_3', 0, \omega)$. This is equivalent to usual assumption in the Lighthill theory, that the source functions can be determined by considering an incompressible flow.

For spectral elements with very low subsonic phase speeds, γ is purely imaginary with a large positive imaginary part. Equation (2.11) then shows that, in this regime, the effect of sources away from the boundary decays exponentially with their distance from the boundary. If, however, the boundary-layer thickness, δ, is small in comparison with $|\gamma|^{-1}$, the exponential terms in the integral in (2.11) are approximately unity, and it is convenient to cast the source terms into non-dimensional form.

The Reynolds stresses, T_{ij}, are proportional to the square of the velocity perturbations, which in turn scale on the friction velocity u_τ. We will non-dimensionalise lengths on the boundary-layer displacement thickness, δ^*, and time on δ^*/U_∞, where U_∞ is the free-stream velocity. Hence

$$\int \tilde{T}_{ijkl}(y_3, y_3', \underline{k}, \omega)\, dy_3 dy_3' = \frac{\rho^2 u_\tau^4 \delta^{*5}}{U_\infty} S_{ijkl}\left(\frac{\omega\delta^*}{U_\infty}\right) \qquad (2.12)$$

where S_{ijkl} is a non-dimensional function of $\omega\delta^*/U_\infty$ only. Equation (2.11) becomes

$$\tilde{P}_R(\underline{k}, \omega) = \frac{d_i^* d_j^* d_k d_l}{|k|^2} \frac{\rho^2 u_\tau^4 \delta^{*5}}{U_\infty} S_{ijkl}\left(\frac{\omega\delta^*}{U_\infty}\right) \qquad (2.13)$$

This result can be used to comment on the limiting forms of the power spectrum of the wall pressure.

For spectral elements with subsonic phase speeds, i.e. for spectral components with $|\omega|/c_0 << k << \delta^{-1}$,

$$\gamma \sim ik \qquad (2.14)$$

and

$$\tilde{P}_R(\underline{k}, \omega) \sim \frac{d_i^* d_j^* d_k d_l}{k^2} \frac{\rho^2 u_\tau^4 \delta^{*5}}{U_\infty} S_{ijkl}\left(\frac{\omega\delta^*}{U_\infty}\right) \qquad (2.15)$$

For these wavenumbers, all the components of $\underline{d}$ depend only on $\underline{k}$ and the power spectral density is proportional to k^2.

For spectral elements with highly supersonic surface phase speeds, $k << |\omega|/c_0$

$$\gamma \sim \omega/c_0. \tag{2.16}$$

The predicted surface pressure spectrum simplifies to

$$\tilde{P}_R(\underline{k}, \omega) \sim \frac{\rho^2 u_\tau^4 \delta^{*3} M^2}{U_\infty} \left(\frac{\omega\delta^*}{U_\infty}\right)^2 S_{3333}\left(\frac{\omega\delta^*}{U_\infty}\right) \tag{2.17}$$

where M is the free-stream Mach number U_∞/c_0. In this limit the wall pressure spectrum becomes independent of wavenumber.

Sevik (1986) collects together experimental data for this highly supersonic regime. He shows that results obtained on a buoyant body in water agree closely with wind-tunnel measurements on both smooth and rough walls, when expressed in the non-dimensional form in (2.17). He fits the curve

$$\tilde{P}_R(\underline{0}, \omega) \sim 5.6 \frac{\rho^2 u_\tau^4 \delta^{*3} M^2}{U_\infty} \left(\frac{\omega\delta^*}{U_\infty}\right)^{-4.5} \tag{2.18}$$

to the experimental data in the frequency range $3 < \omega\delta^*/U_\infty < 30$. This is entirely compatible with the theoretical form in (2.17) and a comparison of the two expressions tells us that

$$S_{3333}(\omega\delta^*/U_\infty) = 5.6\,(\omega\delta^*/U_\infty)^{-6.5} \tag{2.19}$$

Since measured pressure spectra are observed to be "wavenumber white", that is practically independent of $\underline{k}$, for spectral elements with supersonic phase velocities, we might (after an inspection of (2.13)) expect the other components of $S_{ijkl}(\omega\delta^*/U_\infty)$ to be of the same order.

Chase (1987) obtains predictions for hard wall surface pressure spectra. He develops his model from the Lighthill theory by making specific assumptions about the source spectra. Chase's model agrees well with data in the convective and subsonic regime (Blake 1986, figure 8.15). In the supersonic regime his expressions simplify considerably and lead to

FLOW NOISE

$$\tilde{P}_R(0,\omega) = 1.2\times10^{-2}\ \frac{\rho^2 u_\tau^4 M^2 \delta^{*3}}{U_\infty}\left(\frac{u_\tau\delta}{U_\infty\delta^*}\right)^2\left(\frac{\omega\delta^*}{U_\infty}\right)^{-1}, \qquad (2.20)$$

for $\omega\delta^*/U_\infty > 0.1$. It is immediately striking that this prediction has quite a different dependence on frequency from the experimental fit in (2.18). If (following Blake 1986, page 505) we assume that $\delta^*/\delta = 3.6\,u_\tau/U_\infty$, equation (2.20) reduces to

$$\tilde{P}_R(0,\omega) = 9.1\times10^{-4}\ \frac{\rho^2 u_\tau^4 M^2 \delta^{*3}}{U_\infty}\left(\frac{\omega\delta^*}{U_\infty}\right)^{-1}, \qquad (2.21)$$

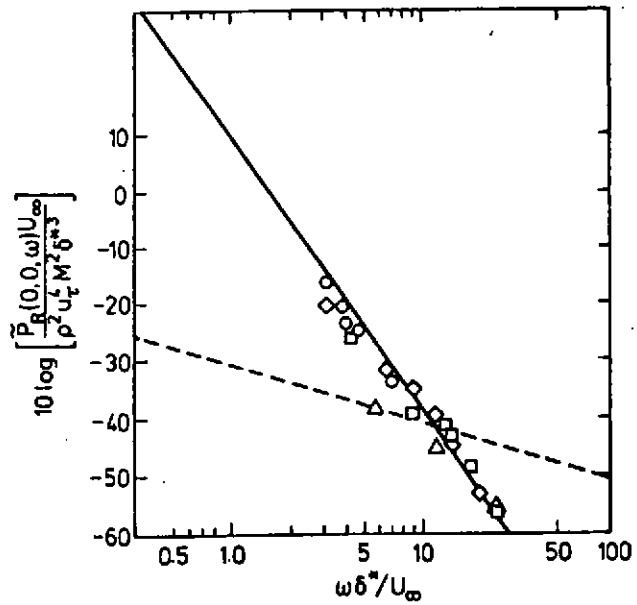

Figure 3 Variation of flow noise with non-dimensional frequency.
_____ Sevik's empirical fit; - - - Chase's model.

The experimental data is from Sevik (1986), 0 buoyant body;
◇ smooth, □ medium rough ($k_s u_\tau/\nu = 50$), △ fully rough ($k_s u_\tau/\nu = 1000$),
wind-tunnel data of Geib & Farabee

and we can obtain a numerical comparison between Chase's predictions and the experimental data. This is shown in Figure 3. Equation (2.21) tends to underestimate the experimental results by about 20dB near $\omega\delta^*/U_\infty = 3$, and overestimate them by some 14dB near $\omega\delta^*/U_\infty = 30$.

Both the theoretical prediction (2.13) and the experimental result (2.18) are proportional to the fourth power of the friction velocity. This is a reminder that the source strength depends strongly on the amplitude of velocity fluctuations. Any device that reduces turbulent velocities is likely to reduce the contribution of the turbulent quadrupoles to flow noise. This opens up exciting new possibilities.

Recent research on drag reduction has lead to the development of 'large-eddy breakup devices' or LEBUs. See Nguyen et al (1984), Bandyopadhyay (1986) or Wilkinson et al (1987) for reviews of this work. LEBUs are thin splitter plates about a boundary-layer thickness in length, which are positioned at a height between 0.4δ and 0.8δ above the wall. Such devices have been shown to lead to local skin-friction reductions of between 15 and 40%, with some reduction in skin-friction persisting over a downstream distance of 100δ - 150δ. This is accompanied by a corresponding decrease in turbulence intensity, turbulent Reynolds stress and integral lengthscale (Westphal 1986; Bonnet, Delville & Lemay 1987; Coustols, Cousteix & Belanger 1987).

It is apparent from equation (2.11) that it is these fluctuating velocities that generate sound in a turbulent boundary layer over a plane wall, and we might hope that an array of LEBUs producing a global reduction in turbulence intensity might lead to a corresponding reduction in noise. Such an argument is clearly an over-simplification. Although the introduction of a LEBU might reduce the strength of the quadrupole sources, the LEBU exerts unsteady forces on the fluid and leads to new dipole sources. These dipoles produce centred waves travelling from the LEBU over the surface with the speed of sound. The installation of LEBUs therefore introduces no additional pressure fluctuations with supersonic surface phase speeds and, for these spectral components, we can expect a reduction in flow noise due to the decrease in the strength of the quadrupole sources, T_{ij}. Encouraging experimental results have been reported by Beeler (1986) and Moller & Leehey (1989). They measured pressure spectra downstream of a LEBU in a turbulent boundary layer and found that the presence of the manipulator reduced the unsteady pressures.

The installation of the LEBU increases the surface pressure spectrum for spectral elements with sonic phase speeds. However there is significant flow noise at

these acoustic wavenumbers even without LEBUs. The increase due to the LEBU is not significant at frequencies higher than about $c_0/30\delta$ (Dowling 1989).

The simple theoretical prediction in (2.13) has a non-integrable singularity for spectral elements with sonic phase speeds, for which $k = |\omega|/c_0$ and $\gamma = 0$. This singularity was investigated by Bergeron (1973) and Ffowcs Williams (1982). It arises due to a two-dimensional form of Olbers' paradox, because the turbulent source region is considered to be of infinite extent and the sound field from each source element does not decrease rapidly enough with distance for the integrated effect to be finite. We will use the methods of Ffowcs Williams (1982) to investigate this scale effect.

If we write $q(\underline{x}, t) = \partial^2 T_{ij}/\partial x_i \partial x_j$ equation (2.1) becomes

$$\frac{\partial^2 p'}{\partial t^2} - c_0^2 \nabla^2 p' = q \,, \tag{2.22}$$

and the solution to this equation satisfying the hard surface boundary condition is:

$$p'(x_1, x_2, 0, t) = \int \frac{q(\underline{y}, t - |\underline{x} - \underline{y}|/c_0)}{2\pi|\underline{x} - \underline{y}|} d^3\underline{y} \,. \tag{2.23}$$

In interpreting the singularities it is sufficient to concentrate on $p'_d(\underline{x}, t)$, the contribution to $p'(\underline{x}, t)$ from distant sources, since the singularities arise due to the integrated effect of these distant sources. As the effect of nearby sources is to be neglected, it will not be possible to deduce the full structure of the pressure distribution as was done in equation (2.11), but instead the origin of the singularities can be highlighted. For the distant sources within the turbulent wall region $\sigma = (y_1^2 + y_2^2)^{1/2}$, is much greater than $|\underline{x}|$ and

$$|\underline{x} - \underline{y}| = \sigma - \frac{\underline{y}.\underline{x}}{\sigma} \,. \tag{2.24}$$

Hence:

$$p'_d(x_1, x_2, 0, t) = \frac{1}{2\pi} \int q\left(\underline{y}, t - \frac{\sigma}{c_0} + \frac{\underline{y}.\underline{x}}{\sigma c_0}\right) \frac{d^3\underline{y}}{\sigma} \,. \tag{2.25}$$

Similarly a simple change of variable gives

FLOW NOISE

$$p_d'(x_1 + \Delta_1, x_2 + \Delta_2, 0, t + \tau) = \frac{1}{2\pi}\int q\left(y_1 + \xi_1, y_2 + \xi_2, y_3', t + \tau - \frac{\sigma}{c_0} + \frac{\underline{y}\cdot}{\sigma c_0}(\underline{x} + \underline{\Delta} - \underline{\xi})\right)\frac{d^2\underline{\xi}\, dy_3'}{\sigma} \tag{2.26}$$

The autospectrum of the surface pressure, $P_{Rd}(\underline{\Delta}, \tau)$, can be obtained from the mean value of the product of equations (2.25) and (2.26):

$$P_{Rd}(\underline{\Delta}, \tau) = \frac{1}{4\pi^2}\int Q\left(\underline{y}, y_3', \underline{\xi}, \tau + \frac{\underline{y}\cdot(\underline{\Delta} - \underline{\xi})}{\sigma c_0}\right)\frac{d^2\underline{\xi}\, dy_3' d^3\underline{y}}{\sigma^2} \tag{2.27}$$

where $Q(\underline{y}, y_3', \underline{\xi}, \tau) = \overline{q(\underline{y},t)\, q(y_1 + \xi_1, y_2 + \xi_2, y_3', t + \tau)}$ is the autocorrelation of q.

The origin of the singularity is now apparent. If the turbulence is homogeneous so that Q is independent of y_1 and y_2, the y_1, y_2 integral in equation (2.27) is unbounded. However, when we insist that there is a patch of homogeneous turbulence of large but finite extent L, so that Q is independent of y_1, y_2 for $\sigma < L$ and vanishes for $\sigma > L$,

$$P_{Rd}(\underline{\Delta}, \tau) = \frac{1}{4\pi^2}\int_{\sigma=c_0/\omega}^{L}\int_{\phi=0}^{2\pi} Q\left(y_3, y_3', \underline{\xi}, \tau + \frac{\underline{y}\cdot(\underline{\Delta} - \underline{\xi})}{\sigma c_0}\right) dy_3\, dy_3'\, d^2\underline{\xi}\, d\phi\, \frac{d\sigma}{\sigma}$$

$$= \frac{\ln(\omega L/c_0)}{4\pi^2}\int_{\phi=0}^{2\pi} Q\left(y_3, y_3', \underline{\xi}, \tau + \frac{\underline{y}\cdot(\underline{\Delta} - \underline{\xi})}{\sigma c_0}\right) dy_3\, dy_3'\, d^2\underline{\xi}\, d\phi \tag{2.28}$$

The lower limit on σ has been set as c_0/ω (Howe 1987) as the far-field approximation in (2.25) will only be valid for large σ.

The wall pressure spectrum due to these extensive acoustic sources is given by the Fourier transform of (2.28).

$$\tilde{P}_{Rd}(\underline{k}, \omega) = \int P_{Rd}(\underline{\Delta}, \tau)\, e^{i k_\alpha \Delta_\alpha + i\omega\tau}\, d^2\underline{\Delta}\, d\tau$$

FLOW NOISE

$$= \ln(\omega L/c_0) \int_{\phi=0}^{2\pi} \tilde{Q}\left(y_3, y_3', \omega \underline{y}/c_0\sigma, \omega\right) \delta(\underline{k} - \omega \underline{y}/c_0\sigma)\, dy_3\, dy_3'\, d\phi \quad (2.29)$$

where $\tilde{Q}(y_3, y_3', \underline{k}, \omega) = \int Q(y_3, y_3', \underline{\xi}, \tau) \exp(ik_\alpha \xi_\alpha + i\omega\tau)\, d^2\underline{\xi}\, d\tau$ is the power spectral density of q. One of the δ-functions can be used to evaluate the φ-integral to give:

$$\tilde{P}_{Rd}(\underline{k}, \omega) = 2\ln(\omega L/c_0)\, \delta(k^2 - \omega^2/c_0^2) \int \tilde{Q}\left(y_3, y_3', \underline{k}, \omega\right) dy_3\, dy_3' \quad (2.30)$$

This shows that there is a δ-function singularity for spectral elements with sonic surface wave speed. The peak is now integrable. For a small-scale experimental facility, its integrated effect may not be large because it depends on the logarithm of the extent of the turbulent source region. Dhanak (1988) shows that surface curvature makes the hard wall pressure spectrum integrable in a similar way.

To summarize, we expect the integrated pressure spectrum level near the sonic condition to depend on the geometry or source size for a hard surface. Sevik (1986) reports that experimentally measured levels at $k = \omega/c_0$ are higher than at supersonic wavenumbers, with "most of the energy arriving at grazing incidence from an upstream direction". There is no such anisotropy in equation (2.30), but it will emerge when we consider mean flow effects in §4.

3. A DOMED SONAR SYSTEM

A sonar dome consists of a light surface over a flooded cavity as shown in Figure 4. If the covering surface is sufficiently light it has little effect on pressure perturbations passing through it and the main effect of the dome arrangement is to ensure that the turbulent sources are held away from the hard surface on which the pressure spectrum is measured.

We saw in §2 that the surface pressure spectrum for spectral elements with subsonic phase speeds decays exponentially with the vertical distance between the surface and the sources. The amplitudes of the elements with supersonic phase speeds are not reduced in this way. The domed sonar system can therefore be used to discriminate against the subsonic modes. It dramatically reduces the convective peak in the surface pressure spectrum without a significant change to propagating acoustic waves, thereby increasing the signal-to-noise ratio.

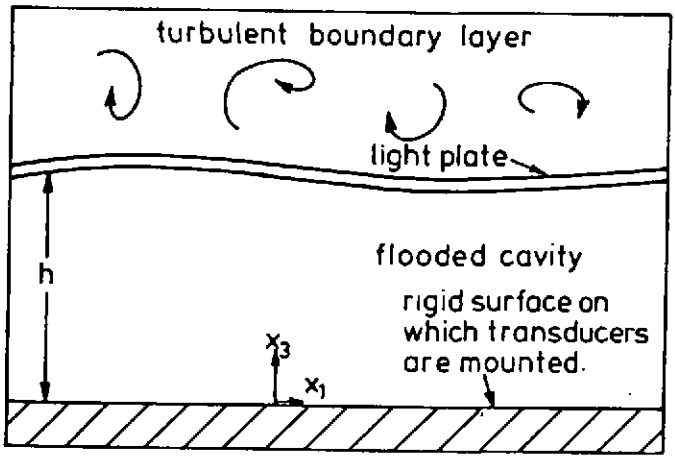

Figure 4 A sonar dome

We can use equation (2.11) as it stands to analyse the performance of a simple dome. We chose our coordinate system so that $x_3 = 0$ is again the hard surface on which the pressure spectrum is measured. If the covering surface is so light that the only effect of a dome of height h is to cause the turbulence to stand off a distance h from the surface $x_3 = 0$, then,

$$\tilde{T}^{D}_{ijkl}(x_3, x_3', \underline{k}, \omega) = \tilde{T}_{ijkl}(x_3 - h, x_3' - h, \underline{k}, \omega), \tag{3.1}$$

where the superscript D denotes the cross-spectral density of the turbulent sources with the dome and $\tilde{T}_{ijkl}$ is their value in the absence of a sonar dome. Substitution into equation (2.11) gives the pressure spectrum on $x_3 = 0$ under a dome of height h as:

$$\tilde{P}_D(\underline{k}, \omega) = \frac{d_i^* d_j^* d_k d_l}{|k|^2} \int_h^\infty \int_h^\infty \tilde{T}^{D}_{ijkl}(y_3, y_3', \underline{k}, \omega)\, e^{i(\gamma y_3' - \gamma^* y_3)}\, dy_3 dy_3' \tag{3.2}$$

After using equation (3.1) and changing the integration variables we see that this can be rewritten as:

$$\tilde{P}_D(\underline{k}, \omega) = \frac{d_i^* d_j^* d_k d_l}{|\gamma|^2} e^{i(\gamma - \gamma')h} \int_0^\infty \int_0^\infty \tilde{T}^D_{ijkl}(z_3, z_3', \underline{k}, \omega) e^{i(\gamma z_3 - \gamma' z_3)} dz_3 dz_3' = e^{i(\gamma - \gamma')h} \tilde{P}_R(\underline{k}, \omega) \tag{3.3}$$

where $\tilde{P}_R(\underline{k}, \omega)$ is the surface pressure spectrum in the absence of the dome. It is apparent from equation (3.3) that the surface pressure spectrum for spectral elements with supersonic phase speeds, for which γ is real, is unaffected by the dome. However the subsonic phase elements, for which $\gamma = i(k^2 - \omega^2/c_0^2)^{1/2}$, are attenuated by a factor:

$$e^{-2(k^2 - \omega^2/c_0^2)^{1/2}h}$$

For highly subsonic modes, $k >> |\omega| / c_0$, and reasonable dome heights this is a considerable reduction. Hence, on a dome-covered surface, flow noise has most effect on the spectral elements of the pressure spectrum with slightly subsonic or supersonic surface wave speeds.

We have considered a very simple model of a dome. This illustrates clearly the very significant attenuation of subsonic elements. However for a more complete analysis of the filtering action of the dome, the mass and stiffness of the covering plate ought to be included. The surface impedance on $x_3 = h$ of the plate and flooded cavity can be calculated in a straightforward way (Maidanik 1968). The flow noise can then be predicted by using the results developed in §5 for general flexible surfaces.

4. MEAN FLOW EFFECTS

So far we have discussed the boundary-layer flow as if it just consisted of turbulence. In practice there is also a mean flow $\underline{U} = (U(x_3), 0, 0)$ parallel to the surface. To account for this it is appropriate to set up Lighthill's equation in such a way that convected derivatives appear in the wave operator and the quadrupole sources T_{ij} involve $\rho v_i' v_j'$, where $\underline{v}'$ is the difference between the fluid velocity and the mean flow $\underline{U}$. That has been done by Lilley (1971). We follow Chase & Noiseux (1982) who show that the equations of mass and momentum conservation can be combined into the form

FLOW NOISE

$$\frac{\partial^2}{\partial x_3^2}\left(\frac{\tilde{\rho}+\tilde{T}_{33}/c_0^2}{\omega+Uk_1}\right)+f\,\frac{\tilde{\rho}+\tilde{T}_{33}/c_0^2}{\omega+Uk_1}=\frac{1}{c_0^2}\left\{\frac{k_\alpha k_\beta\,\tilde{T}_{\alpha\beta}+\gamma^2\tilde{T}_{33}}{\omega+Uk_1}+2ik_\alpha\frac{\partial}{\partial x_3}\left(\frac{\tilde{T}_{\alpha\beta}}{\omega+Uk_1}\right)\right\}. \quad (4.1)$$

In this expression $T_{ij} = \rho v_i' v_j' + (p' - c_0^2\rho')\,\delta_{ij}$, α and β are to be summed over 1 and 2 and the tilde again denotes a Fourier transform.

$$f(x_3, \underline{k}, \omega) = \frac{(\omega+Uk_1)^2}{c_1^2} - k_1^2 - k_2^2 + \frac{d^2U}{dx_3^2}\frac{k_1}{\omega+Uk_1} - 2\left(\frac{dU}{dx_3}\right)^2\frac{k_1^2}{(\omega+Uk_1)^2} \quad (4.2)$$

and $\gamma = ((\omega + U k_1)^2/c_0^2 - k^2)^{1/2}$, with the sign of the square-root chosen so that γ has the same sign as ω when γ is real and $\mathrm{Im}\gamma$ is positive when γ is purely imaginary. In the case of no mean flow equation (4.1) reduces to (2.3).

Outside the boundary layer the fluid is only linearly disturbed from the free stream velocity $(U_\infty, 0, 0)$ and $T_{ij} = 0$. Since disturbances must either decay at large x_3 or be outward propagating sound waves,

$$\frac{\partial\tilde{\rho}}{\partial x_3} = i\gamma_\infty\tilde{\rho} \text{ for large positive } x_3. \quad (4.3)$$

$\gamma_\infty = ((\omega + U_\infty k_1)^2/c_0^2 - k^2)^{1/2}$, is the limit of γ as x_3 tends to infinity. The hard wall boundary condition gives

$$\frac{\partial\tilde{\rho}}{\partial x_3} = 0 \text{ on } x_3 = 0. \quad (4.4)$$

The ordinary differential equation (4.1) is to be solved subject to the boundary conditions (4.3) and (4.4). Standard Green function techniques make it easy to determine the solution. It is convenient to introduce a function $E(x_3)$, which satisfies the homogeneous equation

$$\frac{d^2E}{dx_3^2} + fE = 0, \quad (4.5)$$

together with the boundary conditions

$$\frac{dE}{dx_3} \to i\gamma_\infty E \text{ as } x_3 \to \infty \quad (4.6)$$

and

$$E = 1 \text{ on } x_3 = 0 \tag{4.7}$$

In terms of E the solution to (4.1) is

$$\tilde{p}(0, \underline{k}, \omega) = \frac{\omega}{E'(0) + U'(0)k_1/\omega} \int \left\{ E(y_3) \frac{k_\alpha k_\beta \tilde{T}_{\alpha\beta} + \gamma^2 \tilde{T}_{33}}{\omega + Uk_1} - \frac{\partial E}{\partial y_3} \frac{2ik_\alpha \tilde{T}_{\alpha 3}}{\omega + Uk_1} \right\} dy_3 \tag{4.8}$$

(See Chase & Noiseux (1982) or Dowling (1986) for the derivation of this relationship.)

The function $E(x_3)$ can be evaluated for a particular mean-flow profile by a numerical solution of (4.5). The results in Figure 5 were obtained for a tanh-velocity profile $U(x_3) = U_\infty \tanh(x_3/\Delta)$, where Δ is a measure of the boundary-layer height. But in fact the dominant flow effect does not depend on the details of the boundary-layer profile. That can be seen from an asymptotic solution for $E(x_3)$, valid for low values of the flow Mach number $M = U_\infty/c_0$ and low wavenumbers i.e. $k \sim |\omega|/c_0$.

We seek an expansion for E as a power series in the powers of the Mach number M. To lowest order $E(x_3) = \exp(i\gamma_\infty x_3)$. More algebra is required to obtain the 0(M) term, but it can be shown (Dowling 1986) that

$$E'(0) = i\gamma_\infty (1 + MB) - U'(0)k_1/\omega - 2k_1\omega M\delta^*/c_0. \tag{4.9}$$

δ^* is the boundary-layer displacement thickness, defined by $\delta^* = \int_0^\infty (1 - U(x_3)/U_\infty)dx_3$ B is an order one function. It is evaluated in Dowling (1986), but its precise form does not concern us here.

Substitution for $E(x_3)$ in the representation (4.8) gives

$$\tilde{p}(0, \underline{k}, \omega) = \frac{d_i d_j}{E'(0) + U'(0)k_1/\omega} \int \tilde{T}_{ij}(y_3, \underline{k}, \omega) e^{i\gamma - y_3} dy_3 \tag{4.10}$$

$d_\alpha = k_\alpha$ for $\alpha = 1$ or 2 and $d_3 = \gamma_\infty$. The terms in the numerator cannot all vanish simultaneously and so we have only kept the lowest order terms there. But in the denominator the leading order term can vanish and so terms of order M must be retained.

FLOW NOISE

The wall pressure spectrum, $\tilde{P}_M(k, \omega)$, can be derived from the Fourier transform of the surface pressure in the way outlined in §2, and is given by

$$\tilde{P}_M(k, \omega) = \frac{d_i^* d_j^* d_k d_l}{|E'(0) + U'(0)k_1/\omega|^2} \int \tilde{T}_{ijkl}(y_3, y_3', k, \omega)\, e^{i(\gamma y_3 - \gamma' y_3')}\, dy_3 dy_3'. \qquad (4.11)$$

In the low Mach number limit, equation (4.9) shows that:

$$E'(0) + U'(0)k_1/\omega = i\gamma_\infty (1 + MB) - 2\omega k_1 \delta^* M/c_0. \qquad (4.12)$$

If we neglect terms of order $\omega\delta^*/c_0$ in (4.12), the right-hand side reduces to $i\gamma_\infty$, the uniform mean flow result (Haj Hariri & Akylas 1985). This vanishes for spectral elements with sonic phase speeds. A uniform mean flow has no effect other than to produce a Doppler shift in frequency. The variation in mean-flow velocity leads to the additional terms in (4.12). The profile has most effect on the pressure spectrum near γ_∞, where the leading order term vanishes. Then $i\gamma_\infty MB$ is negligible since both γ_∞ and M are small, and the dominant effect of the mean-flow profile is contained in the term $-2\omega k_1 \delta^* M/c_0$. This is independent of the details of the boundary layer, depending only on its integrated effect through the flow Mach number U_∞/c_0 and the displacement thickness, δ^*. Reutov and Rybushkina (1986) reach the same conclusion from a matching argument.

When the effect of the mean-flow profile is included, the denominator in (4.11) is small near $\gamma_\infty \approx 0$, but it can only vanish when γ_∞ is purely imaginary. Then the first term on the right-hand side of (4.12) is real and negative, and we see from equation (4.12) that $E'(0) + U'(0)k_1/\omega$ can vanish only if ω and k_1 have opposite signs, i.e. for downstream propagating modes. For upstream propagating modes $E'(0) + U'(0)k_1/\omega$ is always non-zero, having a minimum modulus of $2\omega^2\delta^* M/c_0^2$ at $\gamma_\infty = 0$.

The pressure spectrum therefore has a double pole near $\gamma_\infty = 0$ for downstream propagating spectral elements, but it is always finite for upstream propagating elements. This was verified by numerical calculations for a tanh-velocity profile, $U_\infty \tanh(x_3/\Delta)$, and the results are shown in Figure 5. The plot clearly demonstrates that the predicted pressure spectrum is larger for downstream propagating modes with sonic phase speeds than it is for upstream propagating modes. Integration shows that for the tanh-velocity profile $\delta^* = \Delta \log_e 2$, and the

height of the peak for upstream propagating modes in Figure 5 agrees with $-20\log_{10}(2\omega\delta^{*}M/c_0)$, the level predicted from the low Mach number asymptotic theory.

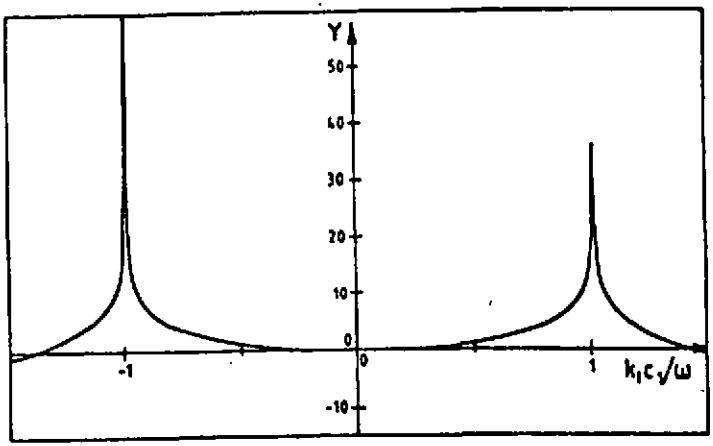

Figure 5 Plot of $Y = 20\log_{10}\left|\frac{\omega/c_1}{E'(0) + U'(0)k_1/\omega}\right|$ versus non-dimensional wavenumber for flow over a rigid wall with $M = 0.01$, $\omega\delta/c_1 = 1$, $k_2 = 0$

Sevik (1986) noted that measurements of pressure spectral elements with sonic phase speeds indicate that most of the energy is propagating downstream in agreement with our predictions.

In Section 2 we found that when the mean-flow profile is neglected, the pressure spectrum has a simple pole for spectral elements with sonic phase speeds. It was possible to interpret the occurrence of these singularities as due to a form of Olbers' paradox: the turbulent source region had been assumed to be of infinite extent and the sound from distant sources did not decay sufficiently rapidly with distance for their integrated effect to be finite. A mean-flow profile enhances the singularity for downstream propagating modes, but eliminates it for upstream propagating modes. Again, this has simple physical interpretation.

When there is a mean-flow profile, there are downstream propagating free modes of the system in which the waves propagate supersonically (i.e. faster than

local sound waves would propagate) within the slowly moving fluid in the boundary layer, but subsonically within the moving fluid outside it. The energy in these modes therefore remains 'trapped' near the wall and conservation of energy then suggests that downstream of a source the pressure disturbance will only decay with the inverse square-root of the distance. Upstream of a source, pressure fluctuations decay much more rapidly. The downstream propagating modes decay more slowly with distance from the source than those in a uniform stream and account for the stronger singularity in the pressure spectrum under an infinite region of turbulence.

In Section 3, we introduced a simple model of a sonar dome. The covering plate was assumed to be so light that it was completely transparent to pressure waves. The main effect of the dome was therefore to produce a stand-off distance, h, between the turbulent sources and the rigid surface on which the pressure spectrum was measured. We will now consider the effect of a mean flow over such a dome.

The effect of a low Mach number mean flow over a hard surface is described by equations (4.11) and (4.12). The term δ^* in (4.12) arises from the integrated effect of the velocity defect $\int_0^\infty (1 - U(x_3)/U_\infty)dx_3$. When there is a dome with a flooded cavity of height h, there is an additional layer in which the mean flow velocity is zero. Hence

$$\int_0^\infty (1 - U(x_3)/U_\infty)\, dx_3 = \delta^* + h \ . \qquad (4.13)$$

The effect of the dome is to increase δ^* in (4.12) to $\delta^* + h$. It therefore decreases the level of the pressure spectrum for modes travelling upstream with the speed of sound. Indeed, the addition of a dome of non-dimensional height $\omega h/c_0 = 5$ to the case shown in Figure 5 reduces the maximum for upstream propagating elements to a level which is only about 20dB larger than the value for highly supersonic modes. With a dome present we would expect the pressure spectrum to be very much larger for downstream propagating modes with sonic phase speeds than it is for upstream propagating modes. Roebuck and Richardson (1981, private communication) have observed this in underwater experiments.

5. FLEXIBLE SURFACES

We have determined the properties of the pressure spectrum induced by turbulence over a hard surface. However, the wavelengths associated with spectral elements with supersonic phase speeds are so long that fluid loading can cause even quite massive surfaces to vibrate. In order to highlight the effects of surface flexibility we will neglect the mean-flow profile and return to the equations and notation of section 2.

The sound generation is described by equation (2.3):

$$\frac{\partial^2 \tilde{p}}{\partial x_\beta^2} + \gamma^2 \tilde{p} = \frac{1}{c_0^2}\left(k_\alpha k_\beta \tilde{T}_{\alpha\beta} + 2ik_\alpha \frac{\partial \tilde{T}_{\alpha 3}}{\partial x_3} - \frac{\partial^2 \tilde{T}_{33}}{\partial x_\beta^2} \right). \tag{5.1}$$

We want to solve this equation, subject to the radiation condition at infinity and a surface boundary condition. We will assume that the turbulent sources, T_{ij}, are uninfluenced by surface flexibility. The surfaces we have in mind are massive (5cm-thick steel plates, for example). While long wavelength sound waves can deform them ($k \sim |\omega|/c_0$), they are effectively rigid to turbulence with its shorter wavelengths ($k \sim \omega/U_\infty$).

Let us suppose that the surface impedance is uniform over the whole surface $x_3 = 0$ and that the relationship between the surface pressure and the normal displacement, $\xi(x_1,x_2,t)$, can be conveniently expressed in terms of their Fourier transforms,

$$\tilde{p}(0, \underline{k}, \omega) = Z(\underline{k}, \omega)\, \tilde{\xi}(\underline{k}, \omega). \tag{5.2}$$

Tensioned membranes, bending plates and more complicated multilayered structures all fall into this category. If the flow near the surface is only linearly disturbed from rest, the linearized momentum equation shows that $\partial \tilde{p}/\partial x_3 = \rho_0 \omega^2 \tilde{\xi}$. Since $\tilde{\rho} = \tilde{p}/c_0^2$, equation (5.2) can be rewritten to give a surface condition for $\tilde{\rho}$.

$$\tilde{\rho}(0, \underline{k}, \omega) = \frac{Z}{\rho_0 \omega^2} \frac{\partial \tilde{\rho}}{\partial x_3}(0, \underline{k}, \omega). \tag{5.3}$$

It is convenient to decompose the density fluctuations into those that occur near a hard wall, with an additional term to account for surface flexibility. We write

FLOW NOISE

$$\tilde{\rho}(x_3, \underline{k}, \omega) = \tilde{\rho}_R(x_3, \underline{k}, \omega) + \tilde{\rho}_F(x_3, \underline{k}, \omega) . \tag{5.4}$$

The rigid wall density fluctuation, $\tilde{\rho}_R\ (x_3, \underline{k}, \omega)$, satisfies equation (5.1) together with the hard wall boundary condition $\partial\tilde{\rho}_R/\partial x_3 = 0$ on $x_3 = 0$. This is precisely the problem solved in Section 2.

When the expansion (5.4) is substituted into (5.1), it shows that $\tilde{\rho}_F$ satisfies a homogeneous equation

$$\frac{\partial^2\tilde{\rho}_F}{\partial x_3^2} + \gamma^2\tilde{\rho}_F = 0 , \tag{5.5}$$

and the boundary condition (5.3) becomes

$$\frac{Z}{\rho_0\omega^2}\frac{\partial\tilde{\rho}_F}{\partial x_3} = \tilde{\rho}_F + \tilde{\rho}_R . \tag{5.6}$$

The problem for $\tilde{\rho}_F$ is straightforward and we find that

$$\tilde{\rho}_F(0, \underline{k}, \omega) = -\frac{\tilde{\rho}_R(0, \underline{k}, \omega)}{1 - i\gamma Z/\rho_0\omega^2} . \tag{5.7}$$

This leads directly to the surface pressure fluctuation

$$\tilde{p}(0, \underline{k}, \omega) = c_0^2\left(\tilde{\rho}_R(0, \underline{k}, \omega) + \tilde{\rho}_F(0, \underline{k}, \omega)\right) \tag{5.8}$$

$$= \frac{i\gamma}{i\gamma - \rho_0\omega^2/Z}\tilde{p}_R(0, \underline{k}, \omega) . \tag{5.9}$$

The power spectral density of the surface pressure, $\tilde{P}(\underline{k}, \omega)$, can be calculated from (5.9) in the way outlined in Section 2:

$$\tilde{P}(\underline{k}, \omega) = \frac{|\gamma|^2}{|i\gamma - \rho_0\omega^2/Z|^2}\tilde{P}_R(\underline{k}, \omega) , \tag{5.10}$$

where $\tilde{P}_R(\underline{k}, \omega)$ is the rigid-wall or 'blocked' pressure spectrum. The multiplying factor $|\gamma|^2/|i\gamma - \rho_0\omega^2/Z|^2$ evidently describes the difference between flexible and rigid wall pressure spectra. After substitution for $\tilde{P}_R(\underline{k}, \omega)$ from (2.13) we obtain

FLOW NOISE

$$\tilde{P}(\underline{k}, \omega) = \frac{d_i^* d_j^* d_k d_l}{|i\gamma - \rho_0\omega^2/Z|^2} \frac{\rho^2 u_\tau^4 \delta^{*5}}{U_\infty} S_{ijkl}\left(\frac{\omega\delta^*}{U_\infty}\right). \quad (5.11)$$

This relates the wall pressure spectrum to source terms which depend on the cross-correlation of the Reynolds stresses. The factor $d_i^* d_j^* d_k d_l / |i\gamma - \rho_0\omega^2/Z|^2$ describes how the turbulent flow radiates sound within the boundary layer over the flexible surface. The product $d_i^* d_j^* d_k d_l$ describes the propagation of different directional elements, but the main structure of the surface pressure spectrum comes from the $|i\gamma - \rho_0\omega^2/Z|^{-2}$ term. We will now investigate the form of the surface pressure spectrum for different surfaces.

As an introductory example we will consider a bending plate backed by a void. For such a surface

$$Z(\underline{k}, \omega) = m\omega^2 - Bk^4, \quad (5.12)$$

where m is the mass of the plate per unit area and $B = Ed^3/12(1-\nu^2)$, E is Young's modulus, ν is Poisson's ratio and d is the plate thickness. In the absence of fluid loading, flexural waves of frequency ω propagate in the plate with a phase speed V equal to $(B\omega^2/m)^{1/4}$. At the coincidence frequency ω_c, V is equal to the sound speed c_0. At frequencies above coincidence V is supersonic and at lower frequencies V is subsonic.

Equation (5.11) shows that the surface pressure spectrum under an infinite extent of turbulence is given by:

$$\tilde{P}(\underline{k}, \omega) = d_i^* d_j^* d_k d_l \, |F(\underline{k}, \omega)|^2 \frac{\rho^2 u_\tau^4 \delta^{*5}}{U_\infty} S_{ijkl}\left(\frac{\omega\delta^*}{U_\infty}\right) \quad (5.13)$$

where

$$F(\underline{k}, \omega) = \frac{m\omega^2 - Bk^4}{\rho_0\omega^2 - i\gamma(m\omega^2 - Bk^4)}. \quad (5.14)$$

An investigation of the form of $F(\underline{k}, \omega)$ will determine the influence of the wall impedance on the surface pressure spectrum. The structure of $F(\underline{k}, \omega)$ depends on N, the Mach number of the in vacuo bending wave speed, V/c_0, and on the

fluid loading factor $\rho_0 c_0/m\omega$, which is essentially the ratio between the mass of fluid within a wavelength of the surface and the mass of the plate. Plots of $F(\underline{k}, \omega)$ are given in Figure 6 for positive ω.

The function $F(\underline{k}, \omega)$ can also be investigated analytically. For heavy plates and highly supersonic spectral elements $F(\underline{k}, \omega) \sim ic_0/\omega$. The pressure spectrum is then identical to the hard surface result in (2.17). It is also apparent from expression (5.14) that $F(\underline{k}, \omega)$ (and hence the pressure spectrum) vanishes for spectral elements whose phase speeds are equal to V. The pressure spectrum has a singularity at $\kappa(\omega)$, a zero of $\rho_0\omega^2 - i\gamma(m\omega^2 - Bk^4)$. For heavy plates $\kappa(\omega)$ can be determined iteratively by an expansion in powers of ρ_0. This shows that there is a singularity in the pressure spectrum near $k = \omega/V$ for $V < c_0$ and near $k = \omega/c_0$ if $V > c_0$ (with the phase speed ω/k just subsonic). These predictions for a heavy plate are confirmed by the plots in Figure 6.

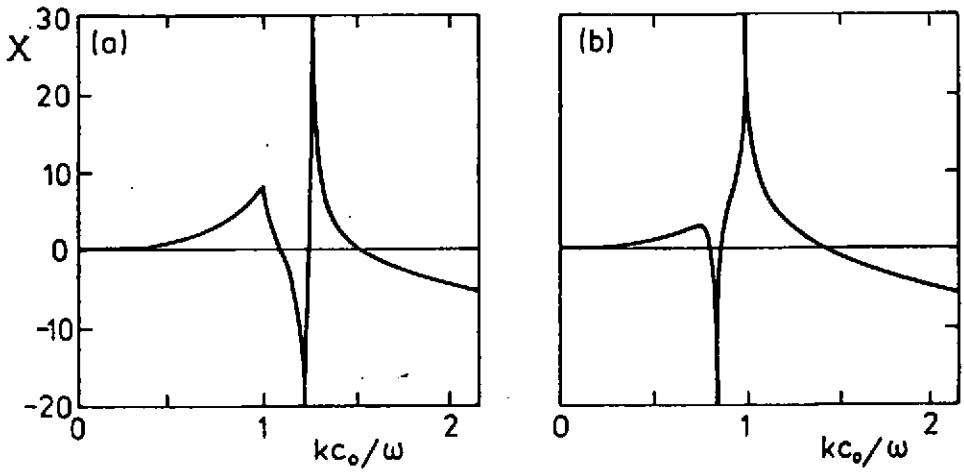

Figure 6 Plots of $X = 20\log_{10}|\omega F(\underline{k}, \omega)/c_0|$ versus non-dimensional wavenumber for a bending plate with a) $m\omega/\rho_0 c_0 = 5$, $N = 0.8$, b) $m\omega/\rho_0 c_0 = 10$, $N = 1.2$

Figure 6 illustrates the variation of $20\log_{10}|\omega F(\underline{k}, \omega)/c_0|$ with non-dimensional wavenumber kc_0/ω. The plate parameters used in these calculations correspond to a 5cm-thick steel plate in water at a frequency of (a) 3kHz and (b) 6kHz. In Figure 6(a), V is subsonic and the singularity in the pressure spectrum occurs for

spectral elements with phase speeds nearly equal to the bending wave speed in vacuo. In Figure 6(b), V is supersonic and the singularity in the pressure spectrum occurs for modes with nearly sonic phase speeds. These singularities are double poles and are stronger than those found for sonic spectral elements on a hard surface. Just as in the hard surface case they arise due to a scale effect, because the source region has been assumed to be infinite.

Since the peaks in the surface pressure spectrum are dominated by the influence of distant sources, the first step in understanding them is to determine the response far from a source adjacent to a bending plate. $\kappa(\omega)$, the zeros of $\rho_0\omega^2 - i\gamma(m\omega^2 - Bk^4)$, are the wavenumbers of free modes of the plate-fluid system. These modes are excited by a source near the surface and travel subsonically over the plate. Since they have a subsonic surface speed they are evanescent in the fluid. All the energy in these modes therefore remains 'trapped' within a disc near the surface and energy conservation suggests that the pressure disturbances associated with the modes should decay like $r^{-1/2}$, where r is the distance from a source near the surface. An asymptotic evaluation of the response due to a point source shows this to be true. This decay rate is slower than that for sound near a hard surface and this leads to stronger singularities in the pressure spectrum. Using the same techniques as in Section 2 to investigate the effect of a finite patch of turbulence shows that there is a δ-function singularity for spectral elements with wavenumber $\kappa(\omega)$. The strength of the δ-function grows linearly with L, the extent of the turbulent source region. The details are given in Dowling (1983).

Although consideration of a finite turbulent source region makes the peaks in the surface pressure spectrum integrable, for reasonably sized source regions, these singularities still have a considerable effect. The integrated pressure level due to the singularities can be significantly larger than the levels elsewhere in the spectrum. Therefore we look for other means of limiting the pressure field.

Howe (1979) investigated the influence of the fluid's viscosity on the pressure spectrum on the hard surface, but found that it only had a small effect. For a flexible surface the wall provides another source of dissipation. The damping in the bending plate will be modelled by giving Young's modulus a small imaginary part. Then $Z(\underline{k}, \omega) = m\omega^2 - Bk^4(1 - i\eta)$, where the damping factor η has the same sign as ω. Plots of $|F(\underline{k}, \omega)|$ with this surface condition are given in Figure 7. As one might expect the damping has most effect on the pressure spectrum for spectral elements whose phase speed is nearly equal to V, the speed of bending waves in the unloaded plate. The pressure spectrum no longer vanishes for spectral components with phase speeds equal to V as it did for the

undamped plate. Also the singularity that occurred near V for frequencies below coincidence is reduced to a reasonable level by dissipation in the plate. The damping has very little effect on the singularity for nearly sonic elements at frequencies above coincidence, essentially because little plate vibration is involved in these glancing modes.

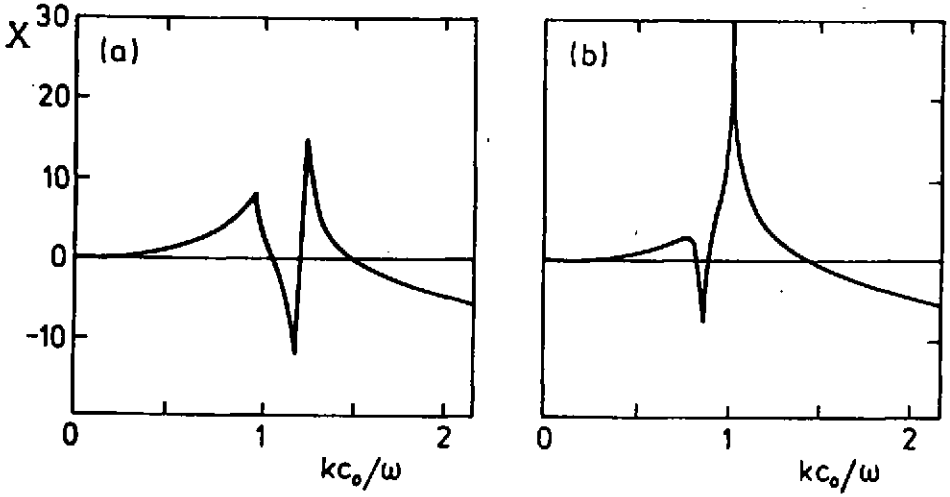

Figure 7 Plots of $X = 20\log_{10}|\omega F(\underline{k}, \omega)/c_0|$ versus non-dimensional wavenumber for a damped bending plate with $\eta = 0.05$ and a) $m\omega/\rho_0 c_0 = 5$, $N = 0.8$, b) $m\omega/\rho_0 c_0 = 10$, $N = 1.2$

There is some experimental evidence that certain surface coatings can also reduce the surface pressure fluctuations due to flow noise. We will model such a coating by a fluid layer of thickness T, with density ρ_s and sound speed c_s. A sketch of the coating is given in Figure 8. The impedance of this composite surface can be found in a straightforward way (Maidanik 1984) leading to $Z(\underline{k}, \omega)$. Equation (5.11) then gives the pressure spectrum on the surface of the coating. In fact the pressure spectrum on the bending plate, $\tilde{P}_B(\underline{k}, \omega)$, is of more practical interest since it can be compared directly with the pressure on the uncoated plate. The relationship between the pressure spectra on these two surfaces can easily be determined and

FLOW NOISE

$$\tilde{P}_B(k, \omega) = d_i^* d_j^* d_k d_l |F_B(k, \omega)|^2 \frac{\rho^2 u_\tau^4 \delta^{*5}}{U_\infty} S_{ijkl}\left(\frac{\omega\delta^*}{U_\infty}\right), \qquad (5.15)$$

and $|F_B(\underline{k}, \omega)|$ is shown in Figures 9 and 10.

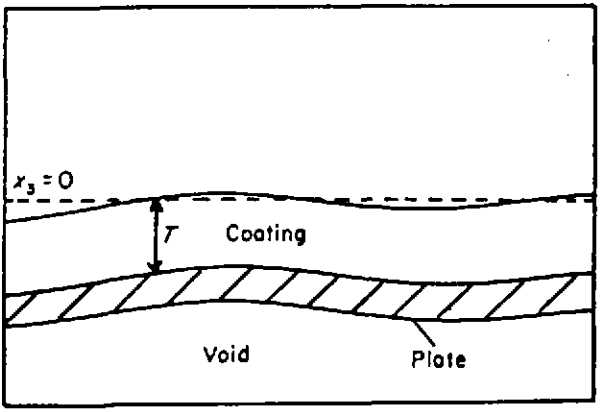

Figure 8 The plate and coating

The coating can have a significant effect on the pressure spectrum for spectral components with sonic phase speeds. If the coating is sufficiently thick and c_s is greater than c_0, it is possible for the coating to control the singularity that would occur for sonic modes in an uncoated plate whenever V is supersonic. The graphs in Figure 9 are for a 4cm-thick coating with $c_s = 1.5c_0$ and $\rho_s = 1.5\rho_0$ on a 5cm-thick steel plate at frequencies of (a) 3kHz and (b) 6kHz. A comparison of Figures 6 and 9 shows that the coating can eliminate the singularity in the spectrum for frequencies above coincidence, but that it has little effect at frequencies below coincidence.

A low sound speed coating with $c_s < c_0$ has an adverse effect on the pressure spectrum generated by the turbulent flow. It can produce a singularity at approximately sonic phase velocities for frequencies below coincidence, where for an uncoated plate the pressure spectrum is not particularly large. Figure 10 shows plots of $|F_B(\underline{k}, \omega)|$ for a 5cm-thick steel plate covered by a 4cm-thick coating layer with $c_s = 0.75c_0$ and $\rho_s = 0.75\rho_0$, again at frequencies of 3kHz and 6kHz. A comparison of Figures 6(a) and 10(a) shows that the low-speed coating has introduced a new singularity not present in the uncoated plate.

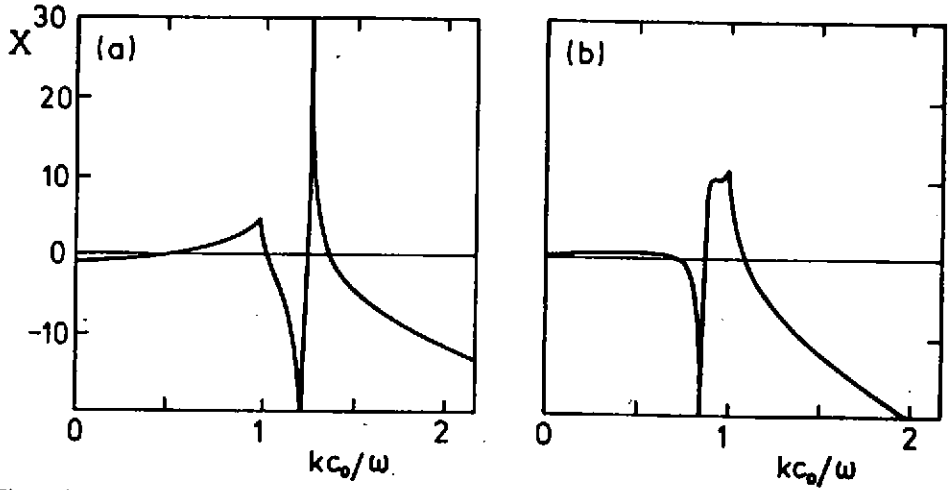

Figure 9 Plots of $X = 20\log_{10}|\omega F_B(\underline{k}, \omega)/c_0|$ versus non-dimensional wavenumber for a coated plate with $c_s = 1.5c_0$, $\rho_s = 1.5\rho_0$ and a) $m\omega/\rho_0 c_0 = 5$, $N = 0.8$, b) $m\omega/\rho_0 c_0 = 10$, $N = 1.2$

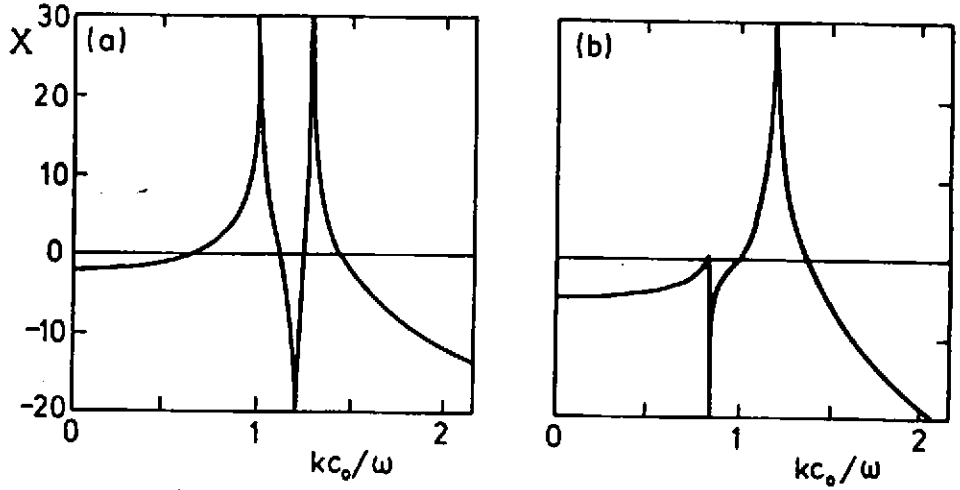

Figure 10 Plots of $X = 20\log_{10}|\omega F_B(\underline{k}, \omega)/c_0|$ versus non-dimensional wavenumber for a coated plate with $c_s = 0.75c_0$, $\rho_s = 0.75\rho_0$ and a) $m\omega/\rho_0 c_0 = 5$, $N = 0.8$, b) $m\omega/\rho_0 c_0 = 10$, $N = 1.2$

FLOW NOISE

So far we have neglected the mean flow when evaluating the pressure spectrum on a flexible surface. Both the mean flow and surface compliance are considered in Dowling (1986). The effect of surface flexibility is to produce an extra term $-\rho_0\omega^2/Z(\underline{k}, \omega)$ in the denominator of (4.11). The relative importance of the mean-flow profile and the surface flexibility is described by the ratio of the two terms $2\omega k_1\delta^* M/c_0$ and $\rho_0\omega^2/Z(\underline{k}, \omega)$. For realistic boundary-layer thicknesses over practical surfaces in water, the effect of the mean-flow profile is small in comparison with the surface flexibility. However, we saw in §3, that a dome can enhance the effect of the mean flow. For a dome of height h over a plate with impedance $iZ(\underline{k}, \omega)/\omega$, we should compare $2\omega k_1(\delta^* + h)M/c_0$ with $\rho_0\omega^2/Z(\underline{k}, \omega)$. It is then possible for the mean flow to have a significant influence.

6. A FINITE PLATE

In this section we outline some current work on the effects of finite surface size. The boundaries of the flexible surface provide an inhomogeneity at which scattering from the convective peak into low wavenumbers can take place. Indeed Crighton (1988) suggests that this wavenumber conversion is the dominant mechanism in sound production by a turbulent boundary layer.

Howe (1988) investigates an infinite bending plate with two line supports a distance a apart. For a steel plate in water with practical supports and $\omega a/c_0 >> 1$, he finds that the principal source of radiation is due to the excitation of flexural modes of the panel by the low wavenumber components of the turbulent sources and their diffraction at the supports. In almost all cases the diffraction of the convective peak leads to terms which are very much smaller. The exception is when the plate displacement is allowed to be discontinuous at the supports(!). Howe found that this extreme boundary condition could produce significant wavenumber conversion.

In Howe's geometry fluid loading enables much of the bending wave energy to be transmitted across the supports. Indeed there is almost perfect transmission at frequencies above coincidence (Howe 1986) and this limits the influence of the finite length of panel. To highlight the effects of finite panel size we will investigate flow noise on a bending plate inserted in an otherwise rigid baffle.

The geometry is illustrated in Figure 11. The plate has a streamwise length a and infinite width, and is mounted in the plane wall $x_3 = 0$. The rest of the wall is rigid. The plate boundaries at $x_1 = 0$ and $x_1 = a$ are simply supported, so that

FLOW NOISE

$$\xi(x_1, x_2, t) = \frac{\partial^2 \xi}{\partial x_1^2}(x_1, x_2, t) = 0 \quad \text{at } x_1 = 0 \text{ and } a\,. \tag{6.1}$$

The plate is excited by a turbulent boundary layer and we wish to find the power spectral density of the surface pressures.

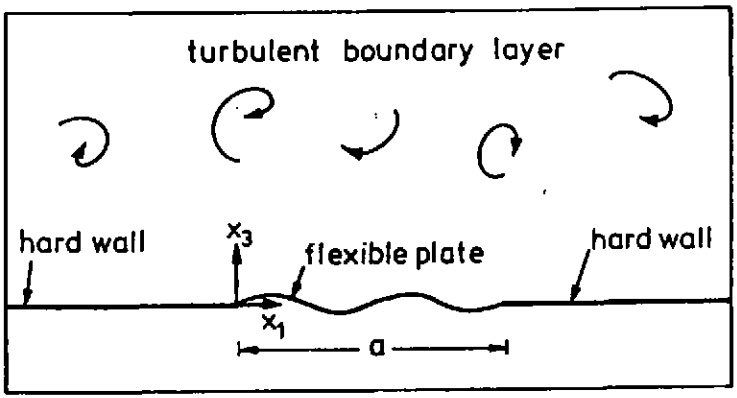

Figure 11 A turbulent boundary layer over a plate of finite length

Lighthill's equation (2.1),

$$\frac{\partial^2 p'}{\partial t^2} - c_0^2 \nabla^2 \rho' = \frac{\partial^2 T_{ij}}{\partial x_i \partial x_j}, \tag{6.2}$$

is to be solved subject to boundary conditions on $x_3 = 0$. The momentum equation shows that

$$\frac{\partial p'}{\partial x_3} = -\frac{\rho_0}{c_0^2}\frac{\partial^2 \xi}{\partial t^2} \text{ for all } x_1 \text{ with } x_3 = 0\,, \tag{6.3}$$

while the equation of motion of the plate leads to

$$\rho' = \frac{1}{c_0^2}\left[-m\frac{\partial^2}{\partial t^2} + B\left(\frac{\partial^2}{\partial x_1^2} - k_2^2\right)^2\right]\xi \quad \text{for } 0 \le x_1 \le a,\ x_3 = 0\,, \tag{6.4}$$

and we have

$$\xi = 0 \quad \text{for } x_1 \ge a \text{ or } x_1 \le 0\,. \tag{6.5}$$

The problem is homogeneous in x_2 and t and it is natural to introduce two-dimensional Fourier transforms:

$$\hat{\xi}(x_1, k_2, \omega) = \int \xi(x_1, x_2, t)\, e^{ik_2x_2 + i\omega t}\, dx_2\, dt\,. \tag{6.6}$$

Transforms of pressure and density can be defined similarly.

In a way analogous to (5.4) we again decompose density and pressure fluctuations into those that occur near a hard wall with an additional term to account for surface flexibility. We write

$$\hat{\rho}(x_1, k_2, x_3, \omega) = \hat{\rho}_F(x_1, k_2, x_3, \omega) + \hat{\rho}_R(x_1, k_2, x_3, \omega) \tag{6.7}$$

The rigid wall density fluctuation, ρ_R, satisfies Lighthill's equation together with the hard wall boundary condition, $\partial\rho_R/\partial x_3 = 0$ on $x_3 = 0$, and was determined in §2. When the expansion (6.7) is substituted into (6.2), it leads to

$$\left(\frac{\partial^2}{\partial x_1^2} + \frac{\partial^2}{\partial x_3^2} + \beta^2\right)\hat{\rho}_F = 0\,, \tag{6.8}$$

where $\beta = (\omega^2/c_0^2 - k_2^2)^{1/2}$. The sign of the square-root is to be chosen such that, when real, β has the same sign as ω and when purely imaginary $\mathrm{Im}\beta$ is positive. It follows from (6.3) that

$$\frac{\partial\hat{\rho}_F}{\partial x_3} = \frac{\rho_0\omega^2}{c_0^2}\hat{\xi} \quad \text{for all } x_1 \text{ with } x_3 = 0\,. \tag{6.9}$$

This problem can be readily rewritten to give $\hat{\rho}_F$ explicitly in terms of the surface displacement $\hat{\xi}$. The solution to (6.8) that satisfies the radiation condition and the boundary condition (6.9) is

FLOW NOISE

$$\hat{\rho}_F(x_1, k_2, x_3, \omega) = \frac{\rho_0 \omega^2}{2ic_0^2} \int_0^a \hat{\xi}(y_1, k_2, \omega)\, H_0^{(1)}(\beta R)\, dy_1 \qquad (6.10)$$

where $R^2 = (x_1 - y_1)^2 + x_3^2$. We need to use the remaining boundary condition (6.4) to determine ξ.

The end conditions in (6.1) suggest that it is convenient to expand $\xi(x_1, k_2, \omega)$ in a Fourier series and we write

$$\xi(x_1, k_2, \omega) = \sum_{M=1}^{\infty} A_M \sin(M\pi x_1/a)\,. \qquad (6.11)$$

The surface density fluctuations are given in terms of the coefficients A_M through equation (6.10):

$$\hat{\rho}_F(x_1, k_2, 0, \omega) = \frac{\rho_0 \omega^2}{2ic_0^2} \sum_{M=1}^{\infty} A_M \int_0^a H_0^{(1)}(\beta |x_1 - y_1|) \sin(M\pi y_1/a)\, dy_1 \qquad (6.12)$$

When this is substituted into the Fourier transform of (6.4) it leads to

$$\sum_{M'=1}^{\infty} \left[m\omega^2 - B(1 - i\eta) \left(\frac{M'^2\pi^2}{a^2} + k_2^2 \right)^2 \right] A_M \sin\left(\frac{M'\pi x_1}{a}\right) = \hat{p}_R(x_1, 0, k_2, \omega)$$

$$+ \frac{\rho_0 \omega^2}{2i} \sum_{M=1}^{\infty} A_M \int_0^a H_0^{(1)}(\beta |x_1 - y_1|) \sin\left(\frac{M\pi y_1}{a}\right) dy_1 \qquad (6.13)$$

for $0 \le x_1 \le a$. The function $\hat{p}_R = c_0^2 \hat{\rho}_R$ denotes the rigid wall pressure fluctuations. A small amount of plate damping, η, has been introduced in this equation. When (6.13) is multiplied by $\sin(N\pi x_1/a)$ and integrated from 0 to a, we obtain an infinite set of coupled equations for the coefficients A_N.

$$\left[m\omega^2 - B(1 - i\eta)\left(\frac{N^2\pi^2}{a^2} + k_2^2\right)^2\right] A_N + \frac{\rho_0\omega^2}{\beta} \sum_{M=1}^{\infty} p_{NM} A_M = \frac{2}{a} \int_0^a \hat{p}_R(x_1, k_2, 0, \omega) \sin\left(\frac{N\pi x_1}{a}\right) dx_1 \tag{6.14}$$

where

$$p_{MN} = \frac{i\beta}{a} \int_0^a \int_0^a H_0^{(1)}(\beta|x_1 - y_1|) \sin\left(\frac{M\pi x_1}{a}\right) \sin\left(\frac{N\pi y_1}{a}\right) dx_1\, dy_1 \tag{6.15}$$

The coupling coefficients p_{MN} have been investigated analytically in the limit $|\beta|a \to \infty$ by Leppington et al (1986) who consider the related problem of sound radiation from an elastic panel excited by a force. They find that while the diagonal terms in p_{MN} can be large, the off-diagonal terms tend to zero as $|\beta|a \to \infty$.

It is therefore natural to rewrite (6.14) in the form

$$\left[m\omega^2 - B(1 - i\eta)\left(\frac{N^2\pi^2}{a^2} + k_2^2\right)^2 + \frac{\rho_0\omega^2}{\beta} p_{NN}\right] A_N + \frac{\rho_0\omega^2}{\beta} \sum_{\substack{M=1 \\ M\neq N}}^{\infty} p_{NM} A_M$$

$$= \frac{2}{a} \int_0^a \hat{p}_R(x_1, k_2, 0, \omega) \sin\left(\frac{N\pi x_1}{a}\right) dx_1 . \tag{6.16}$$

The coupling terms can be expected to be significant for values of M near M_0, the resonance condition at which

$$m\omega^2 - B\left(\frac{M_0^2\pi^2}{a^2} + k_2^2\right)^2 + \frac{\rho_0\omega^2}{\beta} p_{M_0M_0} \approx 0 \tag{6.17}$$

Leppington et al (see their equation (B.9)) derive a solution to (6.16). In our notation it is

FLOW NOISE

$$A_N = \frac{1}{d_N}\left[\frac{2}{a}\int_0^a \hat{p}_R(x_1, k_2, 0, \omega)\sin\left(\frac{N\pi x_1}{a}\right)dx_1 - \frac{\rho_0\omega^2 P_{NM_0}S_f}{\beta + \rho_0\omega^2 PS}\right] \tag{6.18}$$

The parameters in this expression require some explanation. P is the limiting form of p_{MN}, as M and N tend to M_0 with $M \neq N$.

$$P_{NM_0} = \begin{cases} p_{NM_0} & \text{for } N \neq M_0 \\ P & \text{for } N = M_0 \end{cases} \tag{6.19}$$

$$d_N = m\omega^2 - B(1 - i\eta)\left|\frac{N^2\pi^2}{a^2} + k_2^2\right|^2 + \frac{\rho_0\omega^2}{\beta}(p_{NN} - P), \tag{6.20}$$

while

$$S = \sum_{M=1}^{\infty} d_M^1 \tag{6.21}$$

and

$$S_f = \sum_{M=1}^{\infty} \frac{1}{d_M}\frac{2}{a}\int_0^a \hat{p}_R(x_1, k_2, 0, \omega)\sin\left(\frac{M\pi x_1}{a}\right)dx_1 . \tag{6.22}$$

The main contributions to the sums S and S_f will come from values of M near the resonance condition M_0.

We will choose to write the solution to the matrix equation (6.16) in the form

$$A_N = \frac{1}{m\omega^2 a}\sum_{M=1}^{\infty} C_{NM}\int_0^a \hat{p}_R(x_1, k_2, 0, \omega)\sin\left(\frac{M\pi x_1}{a}\right)dx_1 . \tag{6.23}$$

Leppington et al's solution lets us write down immediately the major coefficients C_{NM}. We have

FLOW NOISE

$$C_{NN} = \begin{cases} \dfrac{2m\omega^2}{d_N} & \text{when N is not near } M_0 \\ \dfrac{2m\omega^2}{d_N} - \dfrac{2m\rho_0\omega^4 P}{d_N^2(\beta + \rho_0\omega^2 PS)} & \text{for N near } M_0 \end{cases} \tag{6.24}$$

For M near M_0 the off-diagonal terms are

$$C_{NM} = -\frac{2m\rho_0\omega^4 P_{NM}}{d_N d_M(\beta + \rho_0\omega^2 PS)} \qquad N \neq M \tag{6.25}$$

C_{NM} is, of course, symmetric because the coupling coefficients p_{NM} in (6.15) are symmetric.

We will find later that we are particularly interested in off-diagonal terms C_{NM}, where $M \sim a\omega/\pi U_c$ and $N < a\omega/\pi c_0$. M describes a mode whose phase velocity is close to the eddy convection velocity, U_c, while the mode N has a supersonic phase speed. It is evident from the definition (6.23) that C_{NM} describes surface displacements with wavenumber $N\pi/a$ produced by driving from a pressure field with wavenumber $M\pi/a$. The coefficient p_{NM} is small, and C_{NM} can be determined by an iterative procedure in which the first order solutions in (6.18) are substituted into the sum in equation (6.16) to determine an improved estimate for A_M. This leads to

$$C_{MN} = \begin{cases} -\dfrac{2m\rho_0\omega^4}{d_M d_N \beta} p_{MN} & \text{for N not near } M_0 \\ -\dfrac{2m\rho_0\omega^4}{d_M d_N(\beta + \rho_0\omega^2 PS)} p_{MN} & \text{for N near } M_0 \end{cases} \tag{6.26}$$

After substituting the expansion for A_N in equation (6.23) into (6.12), we obtain an expansion for the Fourier transform of the surface pressure in terms of the hard wall pressure, $\hat{p}_R$.

FLOW NOISE

$$\hat{p}(x_1, k_2, 0, \omega) = \hat{p}_R(x_1, k_2, 0, \omega)$$

$$+ \frac{\rho_0}{2im} \sum_{M=1}^{\infty} \sum_{N=1}^{\infty} C_{NM} \int_0^a \int_0^a \hat{p}_R(x_1, k_2, 0, \omega)\, H_0^{(1)}(\beta|x_1 - y_1|) \sin\left(\frac{M\pi x_1}{a}\right) \sin\left(\frac{N\pi y_1}{a}\right) dx_1\, dy_1 \qquad (6.27)$$

$\hat{p}(x_1, k_2, 0, \omega)$ is the pressure fluctuation on the finite flexible surface. We can use (6.27) to determine the relationship between the power spectral density on the finite plate and that on an infinite hard surface.

The problem is homogeneous in x_2 and t and so in a way analogous to (2.7)

$$\int \overline{p(x_1, x_2, 0, t)\, p(x_1 + \Delta_1, x_2 + \Delta_2, 0, t + \tau)}\, e^{i k_2 \Delta_2 + i\omega\tau}\, d\Delta_2\, d\tau$$

$$= \frac{1}{(2\pi)^2} \int \overline{\hat{p}^*(x_1, k_2, 0, \omega)\, \hat{p}(x_1 + \Delta_1, k_2', 0, \omega')}\, dk_2' d\omega' . \qquad (6.28)$$

The power spectral density of the surface pressure, $\tilde{P}(x_1, \underline{k}, \omega)$, then follows from the transform of this equation with respect to Δ_1,

$$\tilde{P}(x_1, \underline{k}, \omega) = \frac{1}{(2\pi)^2} \int \overline{\hat{p}^*(x_1, k_2, 0, \omega)\, \hat{p}(x_1 + \Delta_1, k_2', 0, \omega')}\, e^{i\Delta_1 k_1}\, d\Delta_1\, dk_2' d\omega' \qquad (6.29)$$

Substitution for $\hat{p}$ from (6.27) into (6.29) leads to $\tilde{P}(x_1, \underline{k}, \omega)$ in terms of the rigid plate power spectral density $\tilde{P}_R(\underline{k}, \omega)$. The rigid plate pressure field is homogeneous. If we assume that the axial correlation length of the turbulence is small in comparison with the plate length a, and that x_1 is not near the ends of the plate, many of the integrals can be evaluated. That leads to

$$\tilde{P}(x_1, \underline{k}, \omega) = \tilde{P}_R(\underline{k}, \omega) + \frac{\rho_0}{2m} e^{ik_1(a/2 - x_1)} \sum \sum C_{NM}^* \tilde{P}_R(\underline{k}, \omega) S_M(k_1)\, I_N^*$$

$$+ \frac{\rho_0 e^{ik_1(a/2 - x_1)}}{2m\gamma} \sum \sum C_{NM} \left[\tilde{P}_R\left(\frac{M\pi}{a}, k_2, \omega\right) e^{iM\pi x_1/a} - \tilde{P}_R\left(\frac{-M\pi}{a}, k_2, \omega\right) e^{-iM\pi x_1/a}\right] S_N(k_1)$$

FLOW NOISE

$$-\frac{\rho_0^2 i e^{ik_1(a/2 - x_1)}}{4m^2\gamma a} \sum\sum\sum\sum C^*_{N'M} C_{MN} \left[D_{MM} \tilde{P}_R\left(\frac{M\pi}{a}, k_2, \omega\right) + E_{MM} \tilde{P}_R\left(\frac{-M\pi}{a}, k_2, \omega\right) \right] S_N(k_1) I^*_{N'} \tag{6.30}$$

where $\gamma = (\omega^2/c_0^2 - k_1^2 - k_2^2)^{1/2}$ and the sums are to be evaluated over positive integers.

$$S_N(k_1) = \left[e^{iN\pi/2} \frac{\sin((k_1 a + N\pi)/2)}{k_1 a + N\pi} - e^{-iN\pi/2} \frac{\sin((k_1 a - N\pi)/2)}{k_1 a - N\pi} \right] \tag{6.31}$$

and

$$I_N = \int_0^a H_0^{(1)}(\beta |x_1 - y_1|) \sin\left(\frac{N\pi y_1}{a}\right) dy_1 \tag{6.32}$$

The coefficients $D_{M'M}$ and $E_{M'M}$ are defined by

$$D_{MM} = E_{MM} = a/4, \tag{6.33}$$

while for $M' \neq M$

$$D_{MM} = -E_{MM} = \begin{cases} 0 & M' - M \text{ even} \\ \frac{a}{2\pi i}\left(\frac{1}{M' + M} + \frac{1}{M' - M}\right) & M' - M \text{ odd} \end{cases} \tag{6.34}$$

The appearance of x_1 on the right-hand side of (6.30) indicates that the finite plate surface pressure spectrum is not homogeneous. For large a the sine-functions in $S_N(k_1)$ are highly oscillatory: the finite plate pressure spectrum varies rapidly with wavenumber, unlike the infinite plate result in (5.10). Such rapid variations are common in problems with finite plates (see, for example, Crocker (1969), Strawderman (1969) and Jacobs et al (1970)).

If we average $\tilde{P}(x_1, \underline{k}, \omega)$ over a wavenumber band Δk, where $\pi/a << \Delta k << \omega/c_0$, and then take the limit $\omega a/c_0 \to \infty$, we recover the infinite plate pressure spectrum. However, for large but finite $\omega a/c_0$, equation (6.30) contains interesting effects which are not apparent in the infinite plate results. There is the possibility of wavenumber conversion with $\tilde{P}(x_1, \underline{k}, \omega)$ being influenced by $\tilde{P}_R(K_1, k_2, \omega)$ with $K_1 \neq k_1$.

FLOW NOISE

We will discuss the interaction between $\tilde{P}_R(K_1, k_2, \omega)$ near the convective peak ($K_1 \sim -\omega/U_c$) and elements of the finite plate pressure spectrum with supersonic phase speeds ($k_1 < c_0/\omega$). This interaction is described by the second and third terms in (6.30)

$$\tilde{P}_1(x_1, \underline{k}, \omega) = -\frac{\rho_0 i e^{ik_1(a/2 - x_1)}}{2m\gamma} \Sigma \Sigma C_{NM} \tilde{P}_R\left(\frac{-M\pi}{a}, k_2, \omega\right) e^{-iM\pi x_1/a} S_N(k_1)$$

$$\frac{-\rho_0^2 i e^{ik_1(a/2 - x_1)}}{4m^2\gamma a} \Sigma\Sigma\Sigma\Sigma C^*_{N'M'} C_{MN} E_{MM} \tilde{P}_R\left(\frac{-M\pi}{a}, k_2, \omega\right) S_N(k_1) I^*_{N'}. \qquad (6.35)$$

We are interested in the contribution to $\tilde{P}_1(x_1, \underline{k}, \omega)$ from summation over all positive integers M', N' and N, but with M restricted so that the wavenumber $M\pi/a$ is of the order of ω/U_c. It is evident that both terms in (6.35) involve C_{NM}, with $M \sim \omega a/(\pi U_c)$. Now an inspection of (6.24) and (6.26) shows that C_{NM} is proportional to $m\omega^2/d_M$ For a 5cm-thick steel plate in water with a frequency of 3kHz and a free-stream velocity of 15m/s, this factor is an incredibly small 4×10^{-9} for $M \sim \omega a/(\pi U_c)$, representing an attenuation of 84dB.

The motivation for evaluating the modal interaction is that near the convective peak $\tilde{P}_R(\underline{k}, \omega)$ is typically 40dB larger than its value for low wavenumbers. However the factor C_{NM} that appears in the interaction terms in (6.35) is so small that scattering from the convective peak into low wavenumbers leads to a contribution to the surface pressure spectrum which is lower than that produced by low wavenumber sources.

The physical interpretation of this result is that the plate is effectively rigid at the convective wavenumber ω/U_c. At this condition the wavelength is so short that bending stiffness ensures negligible plate deflection. Since the pressure field near the convective peak drives little plate vibration, little energy is scattered at the junctions between the plate and the hard wall.

Equation (6.30) displays other effects which are currently under investigation. An infinite plate has a nonintegrable singularity at wavenumbers, $\kappa(\omega)$, of free modes of the plate-fluid system. That singularity is controlled by finite plate size in a way that can be investigated through (6.30). This equation also displays the interaction between these modes and elements with supersonic phase speeds.

This work on finite plates is far from complete. However, we have seen that edge effects do not cause convective turbulent fluctuations to generate a significant contribution to the low wavenumber pressure spectrum.

7. CONCLUSIONS

Investigation of an infinite plate provides insight into many phenomena associated with flow noise. In particular we have summarized the main effects of a sonar dome, a mean-flow profile and surface flexibility on the low wavenumber surface pressure spectrum. Finite surface size introduces considerable complexity. But for steel plates in water at reasonable frequencies, wavenumber conversion from the convective peak does not appear to be a significant source of low wavenumber pressure fluctuations.

ACKNOWLEDGEMENT

I am grateful to the Institute of Acoustics for the honour of the award of the A. B. Wood Medal, and for the invitation to give this lecture. Over the years, I have benefited from discussions with friends and colleagues at the University of Cambridge, the Admiralty Research Establishment, Topexpress Ltd and Ferranti plc. I would like to thank them for their interest and advice.

Parts of the work reviewed here have been carried out with the support of Topexpress Ltd and the Procurement Executive, Ministry of Defence.

REFERENCES

[1] BANDYOPADHYAY, P R, *Trans. ASME I: J. Fluids Engng.*, 108, 127-140 (1986)
[2] BEELER, G B, *AIAA J.*, 24, 689-691 (1986)
[3] BERGERON, R F, *J. Acoust. Soc. Amer.* 54, 123-133 (1973)
[4] BLAKE, W K, 'Mechanics of Flow-Induced Sound and Vibration', Volume II, *Academic Press* (1986)
[5] BONNET, J P, DELVILLE, J and LEMAY, J, 'Proc. Turbulent Drag Reduction by Passive Means', 1, 45-68, *R. Aero. Soc.* (1987)
[6] CHASE, D M, *J. Sound Vib.*, 112, 125-147 (1987)
[7] CHASE, D M and NOISEUX, C F, *J. Acoust. Soc. Amer.*, 72, 975-982 (1982)
[8] CORCOS, G M, *J. Acoust. Soc. Amer.*, 35, 192-199 (1963)
[9] COUSTOLS, E, COUSTEIX, J and BELANGER, J, 'Proc. Turbulent Drag Reduction by Passive Means', 2, 250-289, *R. Aero. Soc.* (1987)

[10] CRIGHTON, D G, *Proc. Instit. Acoustics*, 10, 1-35, (1988)
[11] CROCKER, M J, *J. Sound Vib.*, 9, 6-20 (1969)
[12] DHANAK, M R, *J. Fluid Mech.*, 191, 443-464 (1988)
[13] DOWLING, A P, *J. Sound Vib.*, 88, 11-25 (1983)
[14] DOWLING, A P, *ASME, J. Fluids Engng.*, 108, 104-108 (1986)
[15] DOWLING, A P, *J. Fluid Mech.*, 208, 193-223 (1989)
[16] DOWLING, A P and FFOWCS WILLIAMS, J E, 'Sound and Sources of Sound', *Ellis Horwood* (1983)
[17] FFOWCS WILLIAMS, J E, *J. Fluid Mech.*, 22, 507-519 (1965)
[18] FFOWCS WILLIAMS, J E, *J. Fluid Mech.*, 125, 9-25 (1982)
[19] HAJ HARIRI, H and AKYLAS, T R, *J. Acoust. Soc. Amer.*, 77, 1840-1844 (1985)
[20] HOWE, M S, *J. Sound Vib.*, 65, 159-164 (1979)
[21] HOWE, M S, *IMA J. Applied Maths.*, 36, 247-262 (1986)
[22] HOWE, M S, *Proc. R. Soc. Lond.*, A412, 389-401 (1987)
[23] HOWE, M S, *J. Sound Vib.*, 121, 47-65 (1988)
[24] JACOBS, L D, LAGERQUIST, D R & GLOYNA, F L, *J. Aircraft*, 7, 210-219, (1970)
[25] LEPPINGTON, F G, BROADBENT, E G, HERON, K H, & MEAD, S M, *Proc. R. Soc. Lond.*, A406, 139-171 (1986)
[26] LIGHTHILL, M J, *Proc. R. Soc. Lond.* A211, 564-587 (1952)
[27] LILLEY, G M, *Fluid Dynamics Trans. (Poland)*, 6, 405-420 (1971)
[28] MAIDANIK, G, *J. Acoust. Soc. Amer.*, 44, 113-124 (1968)
[29] MAIDANIK, G, *ASME J. Vib., Acoust., Stress and Reliability in Design*, 106, 369-375 (1984)
[30] MOLLER, J C and LEEHEY, P, *MIT Acoustics and Vibration Laboratory*, Rep. No. 97457-3 (1989)
[31] NGUYEN, V D, DICKINSON, J, JEAN Y, CHALIFOUR, Y, ANDERSON, J, LEMAY, J, HAEBERLE, D, and LAROSE, G, *AIAA-84-0346* (1984)
[32] REUTOV, V P, and RYBUSHKINA, G V, *Sov. Phys. Acoust.*, 32, 217-221, (1986)
[33] SEVIK, M M, 'IUTAM Symp. on Aero- and Hydro- Acoustics, Lyon, France', 285-308, *Springer* (1986)
[34] STRAWDERMAN, W A, *J. Acoust. Soc. Amer.*, 46, 1294-1307 (1969)
[35] WESTPHAL, R V, *AIAA-86-0283* (1986)
[36] WILLMARTH, W W, *Ann. Rev. Fluid Mech.*, 7, 13-38 (1975)
[37] WILKINSON, S P, ANDERS, J B, LAZOS, B S, and BUSHNELL, D M, 'Proc. Turbulent Drag Reduction by Passive Means', 1, 1-32, *R. Aero. Soc.* (1987)